Regularized Partial Phase Synchrony Index Applied to Dynamical Functional Connectivity Estimation

Gaetan Frusque, Julien Jung, Pierre Borgnat, Paulo Gonçalves

▶ **To cite this version:**

Gaetan Frusque, Julien Jung, Pierre Borgnat, Paulo Gonçalves. Regularized Partial Phase Synchrony Index Applied to Dynamical Functional Connectivity Estimation. ICASSP 2020 - IEEE International Conference on Acoustic Speech and Signal Processing, May 2020, Barcelona, Spain. pp.1-5. hal-02459821

HAL Id: hal-02459821
https://inria.hal.science/hal-02459821v1

Submitted on 29 Jan 2020

HAL is a multi-disciplinary open access archive for the deposit and dissemination of scientific research documents, whether they are published or not. The documents may come from teaching and research institutions in France or abroad, or from public or private research centers.

L'archive ouverte pluridisciplinaire **HAL**, est destinée au dépôt et à la diffusion de documents scientifiques de niveau recherche, publiés ou non, émanant des établissements d'enseignement et de recherche français ou étrangers, des laboratoires publics ou privés.

REGULARIZED PARTIAL PHASE SYNCHRONY INDEX APPLIED TO DYNAMICAL FUNCTIONAL CONNECTIVITY ESTIMATION

G. Frusque [⋆], *Student Member, IEEE* , *J. Jung* [†],
P. Borgnat [‡], *Member, IEEE, P. Gonçalves* [⋆] *Member, IEEE* [*]

[⋆] Univ Lyon, Inria, CNRS, ENS de Lyon, UCB Lyon 1, LIP, Lyon, France
[†] HCL, Neuro. Hosp., Functional Neurology and Epileptology Dept & Lyon Neurosc. Res. Cent., INSERM, CNRS, Lyon, France
[‡] Univ Lyon, CNRS, ENSL, UCB Lyon 1, Laboratoire de Physique, Lyon, France

ABSTRACT

We study the inference of conditional independence graph from the partial Phase Locking Value (PLV) index of multivariate time series. A typical application is the inference of temporal functional connectivity from brain data. We extend the recently proposed time-varying graphical lasso to the measurement of partial locking values, yielding a sparse and temporally coherent dynamical graph that characterizes the evolution of the phase synchrony between each pair of signals. Cast as an optimization problem, we solve it using the alternating direction method of multipliers. The approach is validated on simulated Gaussian multivariate signals and Roessler oscillators. The potential of this regularized partial PLV is then illustrated on actual iEEG data during an epileptic seizure.

Index Terms— Phase Locking value, multivariate, dynamical networks, time-varying graphical lasso, iEEG

1. INTRODUCTION

Estimating the underlying network of interaction from a multivariate time series is of great interest for neuroscientists, where the brain can be seen as a nonlinear synchronizing system evolving through time. The functional connectivities (noted FC) are measures of similarities between different signals, e.g. for Electroencephalogram (EEG) recordings, and are used to model the evolving interactions between different areas of the brain. A popular way to identify FC is to measure the phase resemblance between pairs of signals [1]. The resulting so-called Phase Locking Value (PLV) is a measure for bivariate signals that, unfortunately, cannot differentiate direct from indirect connections in the network. In order to remove indirect couplings, an analysis with partial couplings was proposed that leads to the notion of partial Phase Locking Value index (pPLV). The advantage of pPLV is to measure pairwise interactions between signals, irrespective of all possible linear dependencies with other signals (i.e conditional dependencies), spotting thus more direct couplings.

A partial PLV measure was proposed initially in [2]. Similarly to partial correlations, the partial PLV matrix can be expected to be sparse since indirect interactions are eliminated. However, the pPLV estimates, proposed so far, do not entail sparse results. Also, FC in the brain, here estimated as time series built from the recorded signals using sliding temporal windows, ca be expected slow variations between consecutive instants. Henceforth it is relevant to impose both sparsity and smoothness in the estimation of partial PLV indices.

The present work proposes to use the Graphical lasso [3], which produces sparse models from Gaussian correlation matrices, to the context of pPLV. While Graphical lasso was used on spectral density matrices [4], to the best of our knowledge, it has not been considered yet for the measurement of phase synchrony. Also a smoothness constraint will be additionally imposed in the estimation procedures of our pPLV expressions, following the method of time-varying graphical lasso [5, 6], so as to eventually infer a pPLV indices and a dynamical graph, representative of the temporal evolution of the cortical network. The implementation of the proposed time-varying graphical lasso will rely on the alternating direction method of multipliers (ADMM) elaborated in [5], adapted to PLV. We evaluate the performance of our approach, by running the proposed method on Gaussian multivariate signals, and then on signals of Roessler oscillators which are usual benchmarks for non-linear Gaussian signals. Finally, we illustrate the pertinence of smoothed and sparse regularization of partial phase locking values for estimating the functional connectivity from real iEEG signals recorded during an epileptic seizure.

2. BACKGROUND

2.1. Phase Locking Value

Considering L real signal $s_l(t)$, $l \in 1, ..., L$, The Phase Locking Value (PLV) between signals l and l' is a value between 0 and 1, with 0 if there is no phase synchrony between both signals, and 1 if they have identical phases. To introduce the PLV, we need $z_l(t) = a_l(t)e^{i\phi_l(t)}$, the analytic representation of the signals $s_l(t)$, where $a_l(t)$ and $\phi_l(t)$ are the instantaneous amplitude and the instantaneous phase of the signal, respectively. We have $z_l(t) = s_l(t) + i\mathcal{H}(s_l(t))$, with $\mathcal{H}(.)$ the Hilbert transform [7]. Then the PLV matrix, noted $P \in \mathbb{R}^{L\times L}$, is defined as [8]:

$$P_{ll'} = \mid \mathbb{E}_\phi\{e^{i(\phi_l - \phi_{l'})}\} \mid \tag{1}$$

Under ergodic assumptions, an empirical (non parametric) estimate $\hat{P}$ of the PLV matrix can be computed as:

$$\hat{P}_{ll'} = \left|\hat{R}_{ll'}\right| \quad \text{with} \quad \hat{R}_{ll'} = \frac{1}{T}\sum_{t=1}^{T} e^{i(\phi_l(t) - \phi_{l'}(t))} \tag{2}$$

*Supported by the ACADEMICS Grantof the IDEXLYON of the Université de Lyon, PIA ANR-16-IDEX-0005

2.2. Non parametric partial Phase Locking Value

Since the PLV index defined in (1) is a bivariate index, it cannot distinguish between conditionally dependent and conditionally independent interaction of phase synchrony. The partial PLV (noted $pPLV$) is a conditional analysis that ensures that the conditional interactions due to possible linear dependency with other signals are eliminated. In [2] a nonparametric $pPLV$, noted $\hat{Q}$ based on the PLV estimate of Eq. (2), is introduced. Let us first consider the pairwise phase synchronisation matrix $\hat{\mathbf{R}} \in \hat{\mathbb{R}}^{L\times L}$, where the $\hat{R}_{ll'}$ are computed from Eq. (2), (with $\hat{R}_{l'l} = \hat{R}_{ll'}$, and $\hat{R}_{ll} = 1$) and $\mathbf{\Omega} = \hat{\mathbf{R}}^{-1}$ its inverse. The pPLV index between signals l and l' is defined as:

$$\hat{Q}_{ll'} = \frac{\mid \Omega_{ll'} \mid}{\sqrt{\Omega_{ll}\Omega_{l'l'}}} \tag{3}$$

Note that both $\hat{\mathbf{R}}$ and $\mathbf{\Omega}$ are complex matrices. This index is a direct generalization of the partialization analysis done for correlation matrix to obtain the precision matrix [3], or the same partialization for spectral density matrix [4].

3. METHODS

3.1. Graphical lasso on pairwise phase synchronisation matrix

We use graphical lasso (GL) framework to construct our regularised pPLV estimation. Let us consider $X(t)$, $t \in \{1, ..., T\}$, an observation from a L dimensional multivariate Gaussian distribution with zeros mean and covariance matrix $\mathbf{C} \in \mathbb{R}^{L\times L}$. The task of GL is to estimate a regularized inverse covariance matrix, called precision matrix and noted $\mathbf{\Theta}$. This is achieved by minimizing the regularized negative log-likelihood function:

$$\underset{\mathbf{\Theta}\in\mathbb{S}^p_{++}}{\operatorname{argmin}} \; -\ln(\det(\mathbf{\Theta})) + \operatorname{Tr}\left(\mathbf{\Theta}\hat{\mathbf{C}}\right) + \lambda\mathbf{Reg}\left(\mathbf{\Theta}\right) \tag{4}$$

λ is a parameter of trade-of for the convex regularization function $\mathbf{Reg}(\bullet)$, $\hat{\mathbf{C}} \in \mathbb{R}^{L\times L}$ the sample covariance matrix and $\mathbb{S}^p_{++}$ is the set of symmetric positive-definite matrix.

As the minimization problem of Eq. (4) is convex for all semi-definite positive matrices, it can be transposed to other contexts by replacing $\mathbf{C}$ by a different matrix. In particular, we propose here to replace $\hat{\mathbf{C}}$ by the pairwise phase synchronization matrix $\hat{\mathbf{R}}$.

Storing the vectors $(\Phi_l)_{t=1...T} = e^{i\phi_l(t)}$ as the rows of a matrix $\mathbf{\Phi} \in \mathbb{R}^{L\times T}$, we readily get from Eq. (2) that:

$$\hat{\mathbf{R}} = \frac{1}{T}\mathbf{\Phi}\mathbf{\Phi}^*, \tag{5}$$

showing that $\hat{\mathbf{R}}$ is the sample covariance matrix of the phase multivariate signal. The Gaussian hypothesis that led to Eq.(4) is not necessarily valid in the case of $\hat{\mathbf{R}}$, however, this matrix is semi-definite positive. Thus the regularized pPLV index, defined in (3), can have a regularized estimate using (4) so that the matrix $\hat{\mathbf{\Omega}}$ minimizes the following criterion:

$$\underset{\mathbf{\Omega}\in\mathbb{S}^p_{++}}{\operatorname{argmin}} \; -\ln(\det(\mathbf{\Omega})) + \operatorname{Tr}\left(\mathbf{\Omega}\hat{\mathbf{R}}\right) + \lambda\mathbf{Reg}\left(\mathbf{\Omega}\right) \tag{6}$$

The proposed estimator gets the interesting property that if $\lambda = 0$, the minimizer will coincide with the inverse matrix $\mathbf{\Omega} = \hat{\mathbf{R}}^{-1}$.

As forth-mentioned, $\hat{\mathbf{R}}$ is a complex matrix, and the generalization of GL to complex inputs has only been recently considered. In [9], several GL criteria are proposed depending on the properties of the complex multivariate random variables used to model the input. However, in the current applications of complex GL, [4] [10], it boils down to the use of the standard criteria (4) with complex matrices. It corresponds to our proposition Eq (6), but without clear justification. We motivate the use of the complex GL criterion of Eq. (6) by noticing that it is the regularized negative log-likelihood function of the centered multivariate proper circular complex Gaussian distribution:

$$p(\mathbf{z}) = \frac{1}{\pi^2\det(\mathbf{K})}e^{-\mathbf{z}^*\mathbf{K}^{-1}\mathbf{z}} \tag{7}$$

As shown in [8], it corresponds to the distribution of the analytic representation $\mathbf{z}(t)$ of the signal $\mathbf{s}(t)$, when $\mathbf{s}(t)$ is a realisation of an i.i.d centred multivariate Gaussian distribution. In this case, the distribution of Eq. (7) has this plain form because $z(t)$ is a proper and circular complex random variable (with independent imaginary and real part [7]). Then the phase signal $\phi_l(t)$, constructed from $z_l(t)$, shares these two properties, so there is no need to deduce a complex GL criteria from a more complicated complex multivariate Gaussian distribution.

3.2. Time varying graphical lasso for functional connectivity estimation

We are now seeking to adapt the regulation term $\mathbf{Reg}(\bullet)$ to the specific problem of estimating the temporal evolution of functional connectivities in the brain. We only want to focus, in a clinical setting, on the most significant functional connectivities, and a sparse regularization will be imposed on the pPLVs. Then, as we expect the connectives to evolve in a continuous way, constraint of temporal smoothness is added on the optimization problem Eq.(6). This is relevant when computing a regularized pPLV indexes over sliding short-time windows. Morally this amounts to chop the time series $s_l(t)$ into N segments of duration T, i.e. $\{s_l^{(n)}(t),\, n = 1, \ldots, N,\, 0 \le t < T\}$. From this segmentation, the smoothness constraint amounts to impose slowly varying pPLV estimates over adjacent windows. Adding these two constraints to the complex graphical lasso of Eq. (6), leads us to use the time varying graphical lasso [5], where the matrices $\{\mathbf{\Omega}^{(1)}, ..., \mathbf{\Omega}^{(N)}\}$ are solutions of the following optimization problem:

$$\underset{\mathbf{\Omega}^{(1)},\ldots,\mathbf{\Omega}^{(N)}\in\mathbb{S}^p_{++}}{\operatorname{argmin}} \; \sum_{n=1}^{N}\left[-\ln(\det(\mathbf{\Omega}^{(n)})) + \operatorname{Tr}\left(\mathbf{\Omega}^{(n)}\hat{\mathbf{R}}^{(n)}\right)\right.$$
$$\left. +\lambda \parallel \mathbf{\Omega}^{(n)} \parallel_{od,1}\right] + \gamma\sum_{m=1}^{N-1} g\left(\mathbf{\Omega}^{(m+1)} - \mathbf{\Omega}^{(m)}\right). \tag{8}$$

Here, λ and γ are hyper-parameters tuning respectively the sparsity regularization $\parallel \mathbf{\Omega} \parallel_{od,1} = \sum_{i,\, j\neq i} \mid \Omega_{ij} \mid$ and the temporal smoothness. For this latter term, we follow the recommendations in [5], and we use $g(\mathbf{\Omega}) = \sum_{l=1}^{N} \parallel \Omega_l \parallel_F^2$, with $\parallel . \parallel_F^2$ the Frobenius norm, which is a regularization that is claimed to yield stable inferences on dynamical networks. To

solve the optimization problem of Eq. (8), we use the alternating direction method of multipliers (ADMM) developed in [5]. The generalization of this algorithm for complex variables is straightforward, by replacing the signed soft thresholding function by the complex soft thresholding that is still expressed as: $ST(x,\lambda) = \frac{x}{|x|}\max(|\,x\,| - \lambda; 0)$ for $x \in \mathbb{C}$.

Finally, the regularized partial Phase Locking Value estimated from Eq. (8) between the two chopped signals $s_l^{(n)}(t)$ and $s_{l'}^{(n)}(t)$ reads as:

$$\hat{Q}_{ll'}^{(n)}(\lambda,\gamma) = \frac{|\,\hat{\Omega}_{ll'}^{(n)}(\lambda,\gamma)\,|}{\sqrt{\hat{\Omega}_{ll}^{(n)}(\lambda,\gamma)\hat{\Omega}_{l'l'}^{(n)}(\lambda,\gamma)}} \tag{9}$$

4. MODEL AND RESULTS

To validate the proposed estimation procedure, we synthesize different sets of time series $\{s_l^{(n)}(t),\ l = 1,\dots,L,\ n = 1,\dots,N,\ 0 \le t < T\}$ with prescribed temporal evolutions of their pPLV matrices $\mathbf{Q}^{(n)}$.

4.1. Performance of the proposed approach

We start with a toy example composed of three signals $\{s_l^{(n)}(t),\ l = 1,2,3\}$ chopped into $N = 90$ segments of duration $T = 500$ time samples. In order to model coupled oscillation between signals, where the amount of coupling between the connectivity l and l' is noted $\epsilon_{ll'}$, two models of interaction are proposed underneath.

4.1.1. Coupled oscillation with Gaussian model

Let us consider three processes $\eta_i(t)$, realisation of an i.i.d standard normal distribution, and the model is:

$$\begin{aligned} s_1^{(n)}(t) &= \eta_1^{(n)}(t) \\ s_2^{(n)}(t) &= \epsilon_{1,2}^{(n)} s_1^{(n)}(t) + (1-\epsilon_{1,2}^{(n)})\eta_2^{(n)}(t) \\ s_3^{(n)}(t) &= \epsilon_{1,3}^{(n)} s_1^{(n)}(t) + (1-\epsilon_{1,3}^{(n)})\eta_3^{(n)}(t) \end{aligned} \tag{10}$$

In this model, s_1 is directly coupled with s_2 and s_3, whereas s_2 and s_3 are indirectly coupled conditionnaly to the signal s_1. As in real dataset, it is current to assume that the strength of phase synchronization is not constant in a time series, then, for each time series n, the connectivity level is drawn from a uniform distribution $\epsilon_{ll'}^{(n)} \sim \mathcal{U}_{[0.05,0.6]}$, where the upper and the lower bounds correspond to strong and weak phase synchronization, respectively.

4.1.2. Coupled oscillation with Roessler attractor

This model is commonly used for this context [2, 8, 11]. We consider the following system of three Roessler attractors:

$$\begin{pmatrix} \dot{s}_l^{(n)} \\ \dot{x}_l^{(n)} \\ \dot{y}_l^{(n)} \end{pmatrix} = \begin{pmatrix} -w_l x_l^{(n)} - y_l^{(n)} + \sigma\eta_l^{(n)} + \sum_{l'\neq l}\epsilon_{ll'}^{(n)}(s_{l'}^{(n)} - s_l^{(n)}) \\ w_l s_l^{(n)} + \alpha x_l^{(n)} \\ b + (s_l^{(n)} - c)y_l^{(n)} \end{pmatrix} \tag{11}$$

We set the parameter $a = 0.2$, $b = 0.2$, $c = 10$, $w_1 = 1.03$, $w_2 = 1.01$ and $w_3 = 0.99$ and $\sigma = 3.5$. As in the previous case, the phase synchronization is uniformly distributed $\epsilon_{ll'}^{(n)} \sim \mathcal{U}_{[0.05,0.3]}$.

Figure 1(a) displays the temporal pattern of the oscillation couplings, where the connectivity factors ϵ_{13}, ϵ_{23}, ϵ_{12} are alternately set to zero over the time periods $n = 1,\dots 30$, $n = 31,\dots 60$ and $n = 61,\dots 90$. Notice that the Gaussian model of Eq. (10) coincides to the oscillation coupling pattern only when $\epsilon_{23} = 0$. Fig. 1(b) represents the ideal evolution of the matrices $\mathbf{Q}^{(n)}$ (upper off-diagonal terms) with respect to n. Experiments are performed for the two coupling models and pPLV estimates are averaged over 100 independent realizations of the time series. We empirically tuned the hyper-parameters to $\lambda = 0.1$ and $\gamma = 0.5$.

Table 1 presents two scores assessing the estimation performance of pPLV, obtained without any regularization (noted $Q(0,0)$ in the following[1]), with only a sparse regularization ($Q(\lambda,0)$) or with sparse and temporal regularizations ($Q(\lambda,\gamma)$). The first score we consider, is related to the significance level (false-positive) of coupling detection, and reads $\mathbf{SumNeg} = \sum_{(n,l,l'):Q_{ll'}^{(n)}=0} |\hat{Q}_{ll'}^{(n)}|$. For both models, adding a sparse regularization constraint reduces the risk of false-positive, with a noticeably more pronounced improvement in the case of the Roessler model. However, as mentioned in [12], Graphical Lasso suffers from some biases that lead to a systematic under-evaluation of the coupling values, thus turning the actual phase synchronized pairs more challenging to detect. Therefore, we propose a second score that measures the contrast between pPLV values estimated on coupled pairs *vs* uncoupled ones:

$$\mathbf{Contrast} = \hat{m}_{\{Pos\}} - 2\hat{\sigma}_{\{Pos\}} - (\hat{m}_{\{Neg\}} + 2\hat{\sigma}_{\{Neg\}}) \tag{12}$$

This score measures the discrepancy between values in both sets, using as confidence interval, a surrogate based on the empirical mean $\hat{m}$ and the standard deviation $\hat{\sigma}$. Then, for both models, a good contrast (positive) is achieved only when both the sparse and the temporal regularizations are imposed simultaneously.

Figures 1(c)-(e) show the estimated matrices $\hat{\mathbf{Q}}^{(n)}$ (upper off-diagonal terms) for one realisation of the Roessler model, using respectively the three pPLV estimators: $Q(0,0)$, $Q(\lambda,0)$, $Q(\lambda,\gamma)$. The colormap is scaled to be the same for all methods. The $Q(0,0)$ estimator produces erratic pPLV values that result from the random variability of $\epsilon_{ij}^{(n)}$ in all three states. Figure 1(d) clearly shows how the sparsity constraint attenuates the pPLV estimates in the regions of inactive coupling. Also, as mentioned above, the biases induced by GL globally lowers the estimated values. Finally, $Q(\lambda,\gamma)$ displayed in Fig. 1(e), yields a coupling estimation pattern that is very close to that of the ideal activation template $\mathbf{Q}^{(n)}$ of Fig. 1(b). This is a clear illustration of the advantages of joint sparse and temporal regularization for pPLV estimation.

Model	Score	$Q(0,0)$	$Q(\lambda,0)$	$Q(\lambda,\gamma)$
Gaussian	**SumNeg**	6.8	4.6	5.2
	Contrast	-0.08	-0.13	0.02
Roessler	**SumNeg**	14	4	2
	Contrast	-0.18	-0.15	0.11

Table 1: Performance without regularization $Q(0,0)$, with sparse only $Q(\lambda,0)$, and with sparse and temporal regularization $Q(\lambda,\gamma)$ for the Gaussian and the Roessler models.

[1]We drop the $\hat{}$ for simplicity of notation.

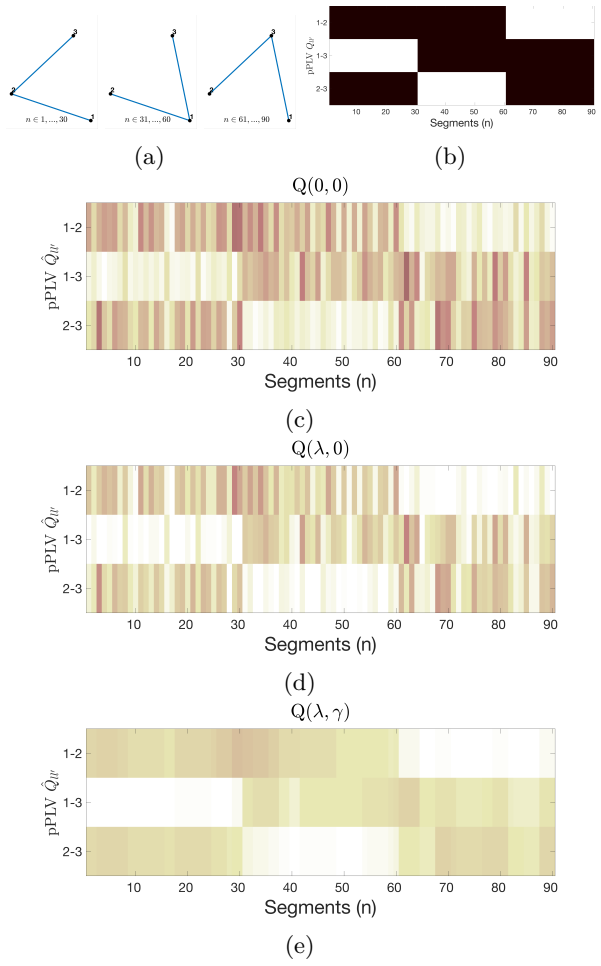

Fig. 1: (a) The 3 connection states for n in different periods. (b) Ideal functional connectivity $\mathbf{Q}^{(n)}$. (c)-(e) Estimated matrices $\hat{\mathbf{Q}}^{(n)}$ (upper off-diagonal terms) for a realisation of the Roessler model, when pPLV is estimated from $\mathrm{Q}(0,0)$, $\mathrm{Q}(\lambda,0)$, and $\mathrm{Q}(\lambda,\gamma)$, respectively.

4.2. Application to iEEG data during seizure

We now consider real iEEG signals, recorded during a seizure of a patient with focal epilepsy [13, 14]. The electrodes used are aligned on stems implanted in the brain. The seizure starts around $t_0 = 50$ sec. and lasts for approximately 87 seconds. The signals are sampled at 256 Hz and we consider only 33 fairly distributed contacts over the initial 108 electrodes, in order to avoid too strong spatial correlations. For the analysis, we use sliding rectangular windows of 2 seconds width, with a one second time step. We end up with the time series $\{s_l^{(n)}(t), n = 1, \dots N, l = 1 \dots L, 0 \leq t \leq T\}$, with $N = 85$ segmets, $T = 521$ sec. and $L = 33$ electrodes. We estimate pPLV without regularization ($Q(0,0)$) and with joint regularization ($Q(\lambda,\gamma)$), to infer the dynamic functional connectivity during the different phases of the seizure. The resulting estimated matrices $\hat{\mathbf{Q}}^{(n)}$ are displayed in Fig 2(a) and Fig 2(b), with $\lambda = 0.3$ and $\gamma = 1$ in this latter case. As expected, the regularized estimator produces much fewer expressed pPLV values. They appear smoother in time, and coincide with the larger pPLV values obtained with the non-regularized estimator of Fig. 2(a). The dynamic of the cortical network becomes easier to segment and to analyse from the reading of the regularized pPLV estimates. In particular, it reveals a synchronous pPLV activation around $n = 50$, conform to the beginning of the seizure.

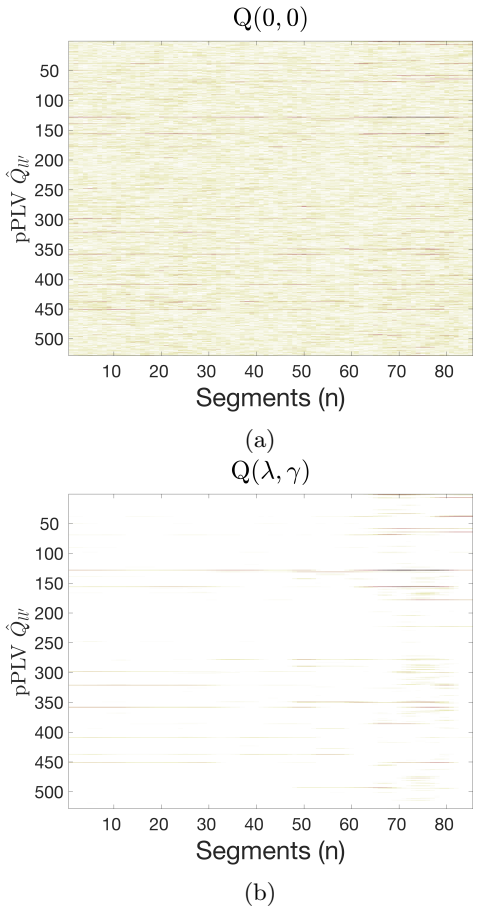

Fig. 2: Estimated matrices $\hat{\mathbf{Q}}^{(n)}$ (upper diagonal elements only) of iEEG recording during a seizure, using the pPLV estimator: (a) without regularization $\mathrm{Q}(0,0)$, and (b): with temporal and sparse regularization $\mathrm{Q}(\lambda,\gamma)$.

5. CONCLUSION

We considered the problem of inferring the conditional independence dynamical graph from the partial phase locking value index (pPLV) of multivariate time series. Since we expect this index to be sparse and smooth in time, we proposed a time varying graphical lasso extension of the pPLV. The regularized pPLV extension was first tested on two different models of oscillatory coupling and then applied to real iEEG data. These numerical examples illustrate the significant advantage of using both types of regularization jointly, to obtain a more robust estimator.

As a follow-up of this work, we are currently investigating a parametric regularized pPLV estimate, assuming that the signals follow a multivariate Gaussian distribution.

6. REFERENCES

[1] P. van Mierlo, M. Papadopoulou, E. Carrette, P. Boon, S. Vandenberghe, K. Vonck, and D. Marinazzo, "Functional brain connectivity from EEG in epilepsy: Seizure prediction and epileptogenic focus localization," *Progress in neurobiology*, vol. 121, pp. 19–35, 2014.

[2] B. Schelter, M. Winterhalder, R. Dahlhaus, J. Kurths, and J. Timmer, "Partial phase synchronization for multivariate synchronizing systems," *Physical review letters*, vol. 96, no. 20, p. 208103, 2006.

[3] J. Friedman, T. Hastie, and R. Tibshirani, "Sparse inverse covariance estimation with the graphical lasso," *Biostatistics*, vol. 9, no. 3, pp. 432–441, 2008.

[4] A. Jung, G. Hannak, and N. Goertz, "Graphical lasso based model selection for time series," *IEEE Signal Processing Letters*, vol. 22, no. 10, pp. 1781–1785, 2015.

[5] D. Hallac, Y. Park, S. Boyd, and J. Leskovec, "Network inference via the time-varying graphical lasso," in *Proceedings of the 23rd ACM SIGKDD International Conference on Knowledge Discovery and Data Mining*. ACM, 2017, pp. 205–213.

[6] P. Danaher, P. Wang, and D. M. Witten, "The joint graphical lasso for inverse covariance estimation across multiple classes," *Journal of the Royal Statistical Society: Series B (Statistical Methodology)*, vol. 76, no. 2, pp. 373–397, 2014.

[7] G. Lindgren, *Stationary stochastic processes: theory and applications*. Chapman and Hall/CRC, 2012.

[8] S. Aydore, D. Pantazis, and R. M. Leahy, "A note on the phase locking value and its properties," *Neuroimage*, vol. 74, pp. 231–244, 2013.

[9] J. K. Tugnait, "Graphical lasso for high-dimensional complex gaussian graphical model selection," in *ICASSP 2019-2019 IEEE International Conference on Acoustics, Speech and Signal Processing (ICASSP)*. IEEE, 2019, pp. 2952–2956.

[10] A. Wodeyar and R. Srinivasan, "Functional connectivity using complex-gaussian graphical models of eeg."

[11] S. Aydore, D. Pantazis, and R. M. Leahy, "Phase synchrony in multivariate Gaussian data with applications to cortical networks," in *2012 9th IEEE International Symposium on Biomedical Imaging (ISBI)*. IEEE, 2012, pp. 1547–1550.

[12] J. Janková and S. van de Geer, "Inference in high-dimensional graphical models," *arXiv preprint arXiv:1801.08512*, 2018.

[13] M. Guenot, J. Isnard, P. Ryvlin, C. Fischer, K. Ostrowsky, F. Mauguiere, and M. Sindou, "Neurophysiological monitoring for epilepsy surgery: the talairach seeg method," *Stereotactic and functional neurosurgery*, vol. 77, no. 1-4, pp. 29–32, 2001.

[14] P. Chauvel, S. Rheims, A. McGonigal, and P. Kahane, "French guidelines on stereoelectroencephalography (seeg): Editorial comment." *Neurophysiologie clinique= Clinical neurophysiology*, vol. 48, no. 1, p. 1, 2018.